Available online at www.sciencedirect.com

ScienceDirect

journal homepage: http://www.elsevier.com/locate/rpor

Original research article

Neutron and high energy photon fluence estimation in CLINAC using gold activation foils

*Kh. Haddad**, *O. Anjak*, *B. Yousef*

Protection & Safety Department, Atomic Energy Commission of Syria, P.O. Box 6091, Damascus, Syria

ARTICLE INFO

Article history:
Received 26 February 2018
Received in revised form 5 July 2018
Accepted 31 August 2018
Available online 11 October 2018

Keywords:
Neutrons
CLINAC
Thermal
Epithermal
Gold
Activation

ABSTRACT

Aim: The thermal neutron, epithermal neutron and high-energy photon fluence were measured in this work around the Varian 21EX 23 MV CLINAC, which is operated in Albairouni hospital in Damascus, Syria.

Background: Photoneutron measurements around medical CLINAC aim to protect both patients and staff from unwanted radiation.

Materials and methods: Neutron and photon activation techniques were applied using gold foils.

Results: It was found that high-energy photons fluence has practically a constant value in the field size. The thermal and epithermal neutron fluence along ox and oy axes has the same order of magnitude.

Conclusion: Gold foils have been used successfully to measure neutron flux and high-energy photons simultaneously using activation techniques.

1. Aim

The aim of this work was to estimate thermal neutron fluence (F_{th}), epithermal neutron fluence (F_{epi}), and high-energy photon fluence (F_{ph}) around the Varian 21EX 23 MV CLINAC, operated in Albairouni hospital, Damascus, Syria using gold activation foils.

2. Background

In radiation therapy with photon energies higher than 10 MeV, neutrons are generated mainly in CLINACs through (γ,n) interactions with nuclei of high atomic number materials constituting the CLINAC head and the beam collimation system.[1–3,17] The radiation activation technique is employed to measure neutrons and high-energy photon fluence in CLINAC.[4,22,25] This technique has been widely used in nuclear reactors and gamma irradiation facilities for the characterization of the high flux of neutron and high-energy gamma photon.[5–7,15] It has the advantage that the detector material can be formed into any shape; they can be large or small depending on the application. Additionally, it can be applied in mixed fields, because it discriminates between different radiations such as gamma photon, neutron, etc.[8] Pure metallic foils are generally used in radiation activation techniques. The foils are activated by radiation. Then the radiation fluence is determined through the measurement of the foil radioactivity. Gold foils were used to measure neutron and high-energy photon in CLINAC.[16,24] Indium foils were used also in radiation activation technique.[14] The neutron fluence around CLINAC was estimated using nuclear track detector.[9] The F_{th}, F_{epi},[19,22]

* *Corresponding author.*
E-mail address: prscientific5@aec.org.sy (Kh. Haddad).

https://doi.org/10.1016/j.rpor.2018.08.009

Table 1 – Characteristics of Gold activation reactions with high-energy photons and neutrons.

Radiation	Interaction		Activation product			Reference
	Type	σ, barns	Nuclide	$T_{1/2}$, d	E, keV	
High-energy photons	(γ,n)	2.19	^{196}Au	6.16	355.73	IAEA[26]
Thermal neutrons	(n,γ)	9.88	^{198}Au	2.69	411.8	[27]
Fast neutrons		7.70				

and F_{ph}[10] around the CLINACs are measured and published for different CLINACs using radiation activation foils.

3. Materials and methods

3.1. *Gold activation detectors*

Gold nuclei interact with high-energy photons and neutrons. These interactions produce radioactive activation products. Table 1 lists the characteristics of gold activation reactions with high-energy photons and neutrons. The flux of high-energy photon and neutron are determined by measurements of the activation product radioactivities. Thus, gold foil can be used to measure high-energy photons and neutrons simultaneously in CLINAC.

3.2. *Neutron flux measurement using gold foil*

The photoneutrons produced in CLINAC have a broad energy spectrum with a high-energy end point of greater than 10 MeV. The majority of the produced neutrons are slowed down in elastic collisions with nuclei of hydrogen in the concrete walls, ceiling and floor. The slowed down neutrons may return to a treatment room and they give their contribution to the specific neutron energy distribution in the vicinity of the accelerator. The thermal and epithermal neutrons fluxes in a position are measured using cadmium ratio technique. Bare gold foils and ones covered by a cadmium sheet were irradiated in the position. The cadmium cover absorbs almost all thermal neutrons. Therefore, the activity of gold foils covered by cadmium is induced by epithermal neutrons.[21] Whereas the activity of bare gold foil is induced by both thermal and epithermal neutrons. HPGe coaxial gamma spectrometer was used to determine ^{198}Au activity induced in each irradiated foil by measuring its characteristic gamma line (411 keV). The cadmium ratio is calculated from experimental data using the relation:[11]

$$R_{Cd} = \frac{A_{tot}}{A_{Cd}} \tag{1}$$

where A_{tot}, A_{Cd} are the measured activities of bare foil and foil covered by cadmium respectively.

To simplify the neutron flux expression the factor F_{Cd} is defined as

$$F_{Cd} = \frac{R_{Cd} - 1}{R_{Cd}} \tag{2}$$

The thermal neutron flux was calculated by:

$$\varphi_{th} = \frac{\exp(\lambda t_d) A_{tot} F_{Cd}}{\sigma_{th} G_{th} N [1 - \exp(-\lambda t_i)]} \tag{3}$$

where A_{tot} is the measured activity of bare foil; λ is the ^{198}Au decay constant; t_d is the foil decay time; t_i is an irradiation time; N is the initial number of ^{197}Au nuclei in the irradiated foil, σ_{th} is the cross section of ^{197}Au(n,γ)^{198}Au reaction for thermal neutrons; G_{th} is the neutron self-shielding factor of the foil for thermal neutrons.

The epithermal neutron flux was calculated by:

$$\varphi_{epi} = \frac{\exp(\lambda t_d) A_{Cd}}{I G_{epi} N [1 - \exp(-\lambda t_i)]} \tag{4}$$

where I is the epithermal integral of the ^{197}Au(n,γ)^{198}Au reaction for epithermal neutrons; G_{epi} is the neutron self-shielding factor of the foil for epithermal neutrons.

Eqs. (3) and (4) were used to determine φ_{th} and φ_{epi} values. The F_{th} and F_{epi} values are obtained simply by multiplying φ_{th} and φ_{epi} by the irradiation time. The effects of foil superficial density in Eqs. (3) and (4) are included by the factors G_{th} as well as G_{epi}. These factors were determined for the used foils.[12]

3.3. *Measurement of high-energy photon flux using gold foil*

High-energy photon flux was measured using Gold foil. The foils were irradiated in the studied positions. HPGe coaxial gamma spectrometer was used to determine ^{196}Au activity induced in the irradiated foils by measuring its characteristic gamma lines (355.7 keV). The high energy photon flux is calculated using the measured ^{196}Au activity by:

$$\phi = \frac{A}{[N\sigma(1 - e^{-\lambda t_{ir}})]} \tag{5}$$

where ϕ is the high-energy photon flux; A is the measured ^{196}Au activity; N is the total number of Gold nuclei in the foil; σ is the high-energy photon activation cross section; λ is ^{196}Au decay constant; t_{ir} is an irradiation period.

This relation can be reduced for short irradiation periods (less than 0.4 half life) by expansion of the exponential term to:

$$\phi = \frac{A}{(N\sigma\lambda t_{ir})} \tag{6}$$

The fluence of particles (neutron or photon) (F) is the number of particles crossing a unit area (1 cm^2), i.e.:

$$F = \phi t_{ir} \tag{7}$$

By rearrangement of Eq. (6) and noting Eq. (7), we get high energies photon fluence:

$$F_{ph} = \phi t_{ir} = \frac{A}{(N\sigma\lambda)} \tag{8}$$

This relation shows that the high-energy photon fluence is a linear function of the measured ^{196}Au activity. This relation was used in this work to estimate the high-energy photon fluence.

3.4. *Measurements*

Pure Gold foils of 99.99% purity, 0.1 mm thickness and 4 mm diameter were used to measure high-energy photon and neutron flux. The mean energy of photoneutron in CLINAC is around several MeV.[23] Thermal neutrons are produced by the interactions with, mainly, hydrogenous materials. Intermediate neutrons are produced by the interactions with medium- and high-Z materials.[13] The Cadmium cover method was applied to separate the thermal neutron.[19]

The foils were irradiated by photon beam of 23 MV Varian linear accelerator type 21EX with field size of 40 cm × 40 cm at Source Axis Distance (SAD) = 100 cm (isocenter level) as shown in Fig. 1. The foils were irradiated for 1.8 min to yield the 6 Gy X-ray dose. The Gold foils were placed, as shown in Fig. 1. The radioactivities of irradiated Gold foils were measured by HPGe gamma-spectrometry. The φ_{th}, φ_{epi} and F were determined using Eqs. (3), (4) and (8) respectively. The F_{th} and F_{epi} was normalized to the therapeutic dose measured by ionization chamber. Such normalization made it possible to render the neutron fluence values independent of a therapeutic beam rate. The peak area uncertainty forms the main component of the total measurement uncertainty. The maximum uncertainty in measurement of the neutron fluence was estimated to be 20%.

4. Results

Tables 2 and 3 list the obtained F_{th}, F_{epi} and F_{ph} in the isocenter respectively along with the corresponding published values in other works. Table 4 lists the obtained F_{ph} in the field size around the isocenter.

Figs. 2 and 3 show the F_{th} and F_{epi} distribution along the ox and oy axis respectively.

Analyzing Table 2 shows the following:

- F_{th} and F_e values are more than the corresponding value in Varian CLINAC-2300, 20 MV;
- F_{th} and F_e values increase as the nominal potential of the therapeutic X-ray beam increases.

These results are interpreted as follows. The cross-section of the photonuclear reactions has an epithermal character. The maximum cross section relates to photon energy of 22 MeV for the low atomic number and to 14 MeV for heavy nuclei. Thus, the photonuclear reactions can be induced in all materials inside the 23 MV X-ray beam whereas in the case of the 20 MV beam these reactions take place mainly in the high atomic number isotopes.[18]

Analyzing Tables 3 and 4 shows the following:

- F_{ph} value has the same order of the corresponding value in CLINAC 2100C 18 MV. However, it is less. This is because the field size in our work is more than that of the other;
- F_{ph} has practically a constant value in the in the field size of 40 × 40 cm^2 around the isocenter. This result is similar to the published one.[20]

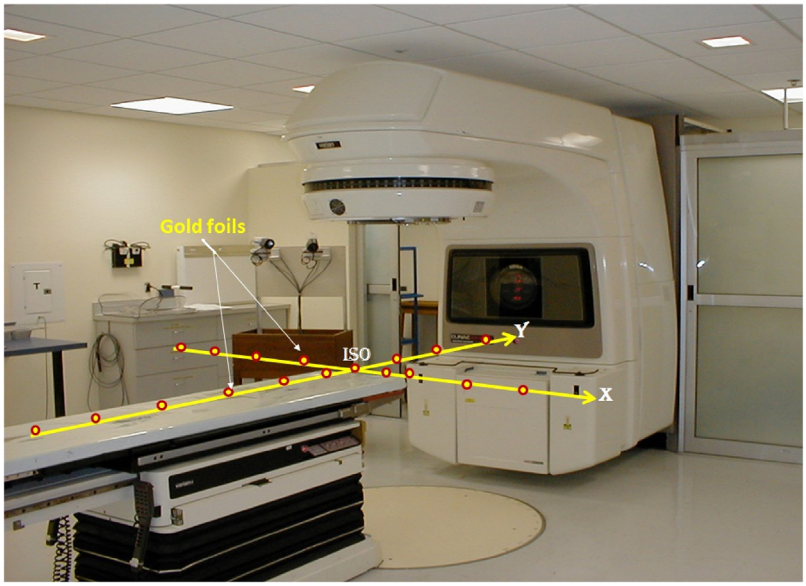

Fig. 1 – Locations of Gold foils in experimental arrangement around the CLINAC at isocenter level.

Table 2 – The measured fluence of thermal and epithermal neutron in the isocenter of Varian 21EX 23 MV CLINAC along with the corresponding published values in other Varian CLINACs.

Varian model	X-rays beam	Radiation field	F_{th}, n cm^{-2}/Gy	F_e, n cm^{-2}/Gy	Reference
Clinac 21EX	23 MV	40 cm × 40 cm	1.88×10^6	5.5×10^5	This work
Clinac-2300	20 MV	10 cm × 10 cm	1.5×10^6	1.2×10^6	[10]
Clinac-2300	15 MV	10 cm × 10 cm	3.0×10^5	2.7×10^5	
Clinac 21EX	10 MV	20 cm × 20 cm	1.46×10^4	–	[22]

Table 3 – The measured fluence of high-energy photon in the isocenter of Varian 21EX 23 MV CLINAC along with the corresponding published value in other Varian CLINAC.

Varian model	Beam	Radiation field	F, ph cm^{-2}/Gy	Reference
Clinac 21EX	23 MV	40 cm × 40 cm	1.45E+09	This work
Clinac2100C	18 MV	10 cm × 10 cm	4.25E+09	[10]

Table 4 – The high-energy photon fluence distribution in the in the field size of 40 × 40 cm^2 around the isocenter.

x	0	0	40	−40
y	40	−40	0	0
Φ, ph/Gy	1.55E+09	1.56E+09	1.52E+09	1.58E+09

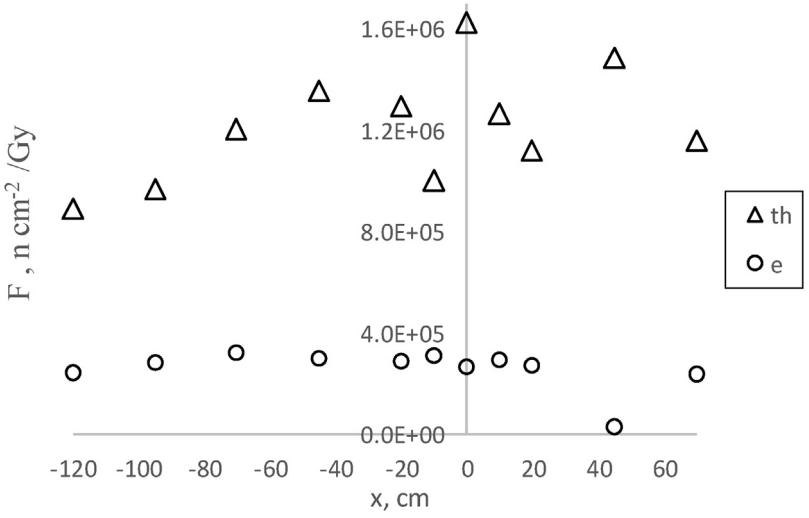

Fig. 2 – Thermal and epithermal neutron fluence distribution along ox axis.

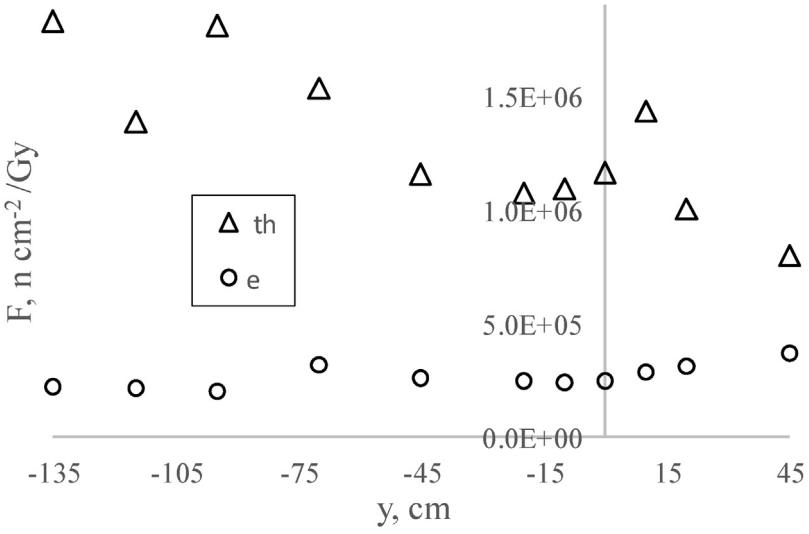

Fig. 3 – Thermal and epithermal neutron fluence distribution along oy axis.

Analyzing Figs. 2 and 3 shows the following:

- F_{th}, F_e values along ox and oy axes have the same order of magnitude. Thus, neutrons can activate the accelerator accessories. Therefore, the accelerator accessories and other massive objects should not be stored in the treatment room.

5. Conclusions

The thermal neutron, epithermal neutron and high-energy photon fluences around the Varian 21EX 23 MV CLINAC have been measured in this work using Gold activation foils. It was found that high-energy photon fluence has practically a constant value in the field size. The thermal and epithermal neutron fluences along ox and oy axes have the same order of magnitude. The results agree with the published one for similar CLINACs and consolidate the fact that, neutron fluence around the CLINAC increases as the nominal potential of the therapeutic X-ray beam increases. The results provide experimental data for the studied CLINAC.

Conflict of interest

There is no conflict of interest statement.

Financial disclosure

There is no grants or financial support other their the institution user the research has her done(Atomic Energy Commission of Syria).

Acknowledgements

The authors would like to thank Prof. I. Othman, the Director General of the Atomic Energy Commission of Syria (AECS); Director General of Albairouni hospital; Prof. M.S. Al-masri, the head of Protection & Safety Department (AECS) and Varian 21EX 23 MV CLINAC staff for the support.

REFERENCES

1. Vega-Carrillo HR, Martínez-Ovalle SA, Lallena AM, Mercado GA, Benites-Rengifo JL. Neutron and photon spectra in LINACs. *Appl Radiat Isotop* 2012;**71**:75–80.
2. Amgarou K, Lacoste V, Martin A. Experimental characterization of the neutron spectra generated by a high-energy clinical LINAC. *Nucl Instrum Methods Phys Res A* 2011;**629**(2011):329–36.
3. Al-Ghamdi H, Fazal-ur-Rehman, Al-Jarallah MI, Maalej N. Photoneutron intensity variation with field size around radiotherapy linear accelerator 18-MeV X-ray beam. *Radiat Meas* 2008;**43**(1):495–9.
4. Szydlowski A, Jaskola M, Malinowska A, Pszona S, Wysocka-Rabin A, Korman A, et al. Application of nuclear track detectors as sensors for photoneutrons generated by medical accelerators. *Radiat Meas* 2013;**50**:74–7.
5. Haddad Kh. Passive nondestructive burnup monitoring of MNSR irradiated fuel by measuring fission products induced photoneutrons. *Appl Radiat Isotop* 2009;**67**(10):1925–9.
6. Haddad Kh, Kattan M, Al Taleb A. Measurement of ^{60}Co high gamma dose using gamma activation of ^{115}In and ^{111}Cd foils. *Appl Radiat Isotop* 2011;**69**(1):180–3.
7. Haddad Kh, Alsomel N. Monitoring of MNSR operation by measuring subcritical photoneutron flux. *Appl Radiat Isotop* 2011;**69**:623–8.
8. Vagena E, Stoulos S, Manolopoulou M. Analysis of improved neutron activation technique using thick foils for application on medical LINAC environment. *Nucl Instrum Methods Phys Res Sect A: Acceler Spectrom Detect Assoc Equip* 2016;**806**:271–8.
9. Shweikani R, Anjak O. Estimation of photoneutron intensities around radiotherapy linear accelerator 23-MV photon beam. *Appl Radiat Isotop* 2015;**99**:168–71.
10. Vagena E, Stoulos S, Manolopoulou M. Geant4 simulations on medical Linac operation at 18 MV: Experimental validation based on activation foils. *Radiat. Phys. Chem* 2016;**120**:89–97.
11. IAEA. *Technical Reports Series No. 107, Neutron Fluence Measurements, Vienna*; 1970.
12. Haddad Kh, Haj-Hassan H, Helal W. Pure commercial gold foils as neutron flux monitor: neutron self-shielding assessment. In: *International conference on research reactors: safe management and effective utilization Sydney*. 2007.
13. Chu WH, Lan JH, Chao TC, Lee CC, Tung CJ. Neutron spectrometry and dosimetry around 15 MV linac. *Radiat Meas* 2011;**46**(12):1741–4.
14. Marcin B, Adam K, Jacek W, Andrzej O. Measurements of thermal and epithermal neutron fluence and induced radioactivity inside bunkers of medical linear accelerators in the center of oncology in Opole, Poland. *Acta Phys Polon B* 2016;**47**(3):771–6.
15. Omar H, Haddad Kh, Ghazi N, Alsomel N. Experimental and operational validation of burn-up calculations for the Syrian MNSR. *Prog Nucl Energy* 2010;**52**(8):753–8.
16. Adam K, Marcin D, Wiktor Z, Włodzimierz Ł, Katarzyna S. Thermal and epithermal neutrons in the vicinity of the Primus Siemens biomedical accelerator. *Nukleonika* 2005;**50**(2):73–81.
17. Adam K, Andrzej O, Marcin D, Zbigniew M, Kinga P-G, Wiktor Z. Correlation between radioactivity induced inside the treatment room and the undesirable thermal/epithermal neutron radiation produced by LINAC. *Phys Med* 2008;**24**(4):212–8.
18. Adam K, Kinga P-G, Wiktor Z. Undesirable nuclear reactions and induced radioactivity as a result of the use of the high-energy therapeutic beams generated by medical LINACs. *Radiat Protect Dosim* 2008;**128**(2):133–45.
19. Adam K, Andrzej O, Marcin Ł, Aleksander C, Marek S. Thermal and epithermal neutrons generated by various electron and X-ray therapeutic beams from medical LINACs installed in polish oncological centers. *Rep Pract Oncol Radiother* 2012;**17**(6):339–46.
20. Adam K, Marzena B, Andrzej O, Zbigniew M, Marek S. Energy spectra in water for the 6 MV X-ray therapeutic beam generated by CLINAC-2300 linac. *Radiat Meas* 2015;**72**:12–22.
21. Adam K, Andrzej O, Marcin B. Measurements of neutron radiation and induced radioactivity for the new medical linear accelerator, the Varian TrueBeam. *Radiat Meas* 2016;**86**:8–15.
22. Wen-Shan L, Sheng-Pin C, Lung-Kwang P, Hsien-Chun T, Chien-Yi C. Thermal neutron fluence in a treatment room with a Varian linear accelerator at a medical university hospital. *Radiat. Phys. Chem* 2011;**80**(9):917–22.
23. Alireza N, Asghar M. A review on photoneutrons characteristics in radiation therapy with high-energy photon beams. *Rep Pract Oncol Radiother* 2010;**15**:138–44.

24. Fujibuchi T, Obara S, Sato H, Nakajima M, Kitamura N, Sato T, et al. Estimate of photonuclear reaction in a medical linear accelerator using a water-equivalent phantom. *Prog Nucl Sci Technol* 2011;**2**:803–7.
25. Haluk Y, İbrahim Ç, Asuman K, Alptuğ Özer Y, Vildan K. Measurement of photo-neutron dose from an 18-MV medical linac using a foil activation method in view of radiation protection of patients. *Nucl Eng Technol* 2016;**48**(2):525–32.
26. IAEA. *IAEA-TECDOC-1178, Handbook on photonuclear data for applications: cross-sections and spectra* IAEA, VIENNA; 2000. p. 2000.
27. www.ndc.jaea.go.jp.